DIGITAL ZENITH CAMERA FOR VERTICAL DEFLECTION DETERMINATION

[1]Māris.Abele, [2]Jānis.Balodis, [3]Inese.Janpaule, [4]Ieva Lasmane, [5]Augusts.Rubans, [6]Ansis.Zariņš

Institute of Geodesy and Geoinformatics, the University of Latvia,
Raiņa bulvāris 19, LV-1586, Rīga, Latvia
E-mails: [1]maris.abele@lu.lv, [2]janis.balodis@lu.lv, [3]inesej@inbox.lv, [4]ieva9lasmane@gmail.com,
[5]augusts.rubans@lu.lv, [6]ansiszx@inbox.lv (corresponding author)

Abstract. Recent advances in accurate astrometric reference star catalogues, development of digital imaging technology, high accuracy tiltmeter technology, and , most af all, geocentric coordinate availability using GNSS have made possible accurate, fast and automated determination of vertical deflections using astrometric methods. Zenith cameras for this kind of measurements have been developed or are being developed by a number of research groups. The paper describes a research project by Institute of Geodesy and Geoinformatics of the University of Latvia, intended to design a portable digital zenith camera for vertical deflection determination with 0.1" expected accuracy. Camera components are described, proposed data processing algorithm and preliminary results, obtained with prototype instrument, are presented.

Keywords: digital zenith camera, GNSS coordinates, geodetic astronomy, vertical deflections, plumb line, geoid.

1. Introduction

Detailed knowledge of local geoid surface recently has become increasingly important in order to fully use the potential of accurate geocentric positions, provided by GNSS. Along with gravimetry, astrometric determination of vertical (plumb line) deflections can give important contribution in determination of local geoid properties (Featherstone, Rüeger 2000; Featherstone, Lichti 2009). Recent advances in a number of scientific and technological fields (accurate astrometric reference star catalogs, development of digital imaging technology, high accuracy tiltmeter technology, and , most of all, geocentric coordinate availability using GNSS) have made it possible to use astrometric methods for accurate, fast and automated determination of vertical deflections. Zenith cameras for this kind of measurements have been developed or are being developed by a number of research groups (Hirt 2006; Hirt, Flury 2008; Hirt et al. 2010; Kudrys 2007, 2009; Ogriznovic 2009, Halicoglu et.al. 2012). However, their number and accessibility are still small. This paper outlines our intended contribution to the area. The project was started in 2010, the goal of it is to design a portable, cheap and robust instrument of this type, using standard components as much, as possible.

2. Camera construction

All digital zenith cameras share basically the same construction principles - they consist of optical tube with imaging device (usually a CCD assembly) on a mount, which can be rotated around vertical axis, equipped with precision tiltmeter, preferably biaxial. Our

design (fig. 1) is similar - the prototype camera uses a 20 cm catadioptric telescope with 1390 mm focus distance, imaging device has 1350x1024 square 6.45 mkm pixels, covering field of 0.35 x 0.27 dg (resolution 0.95" per pixel, image area 0.1 sq. dg.). The final construction will use slightly bigger optics (a 8" catadioptric telescope with focus distance of 2000 mm) and imaging device (3300x2500 5.4 mkm pixels; 0.56"/pixel; 0.5 x 0.39 dg field). Telescope stands on a flat horizontal support surface, on 3 small precision bearings, and can be rotated around vertical axis by any angle using a stepper motor. Tiltmeter is mounted on telescope barrel. Eventually rotating part will have a battery power source and will communicate with control computer using a wireless (WiFi) communication device, however, presently tests are being done using wired connections.

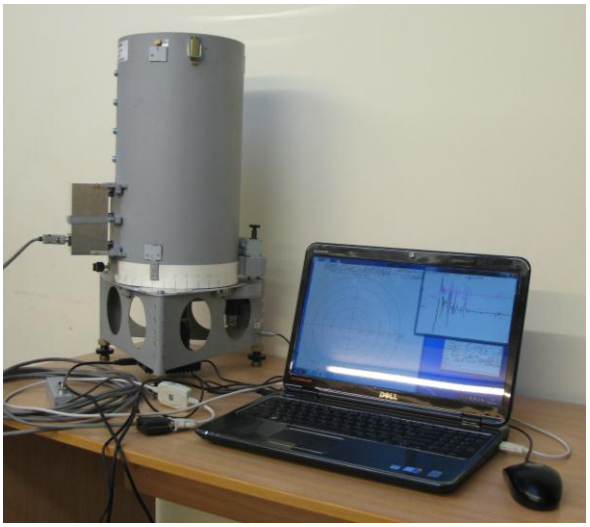

Fig. 1. Prototype zenith camera

Images, obtained by prototype instrument (in rather unfavorable conditions in the center of a city: smog; heavy background illumination from city lights, vibrations caused by transport and other nearby activities) show stars of up to 13^m magnitude for 0.1 sec exposition, we hope to get at least 14^m with the final hardware configuration. In our experience, at least about 20 reference stars per frame are needed for optimal determination of frame position. Taking into account variations in star density distribution in the sky (fig. 2), 12^m is enough for 20 stars per frame at 0.1 sq.dg. field of view during the denser sky period (which occurs to be during spring and summer in our location), 14^m is needed to ensure 20 stars per such frame in any time. Such star magnitude limits also mean, that Hypparcos and Tycho2 catalogs (Høg et.al. 2000) are not sufficient, more extensive (and, unfortunately, also less accurate) catalogs, like UCAC2, USNO-B (Monet et.al. 2003) or NOMAD (Zacharias et.al. 2005) must be used.

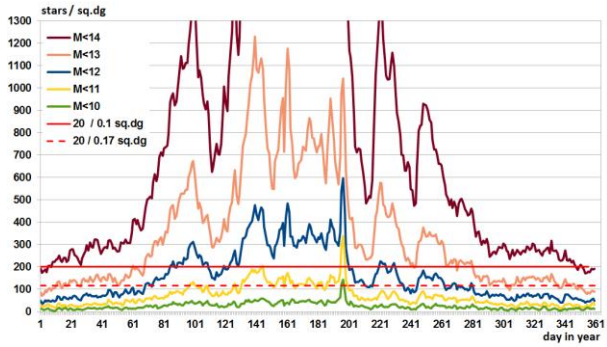

Fig. 2. Star distribution density near zenith at midnight UT for site with 57 dg latitude and 24 dg longitude

Frame exposure moment is obtained referring the pulse, which starts the imaging process, to GPS time scale. Timing accuracy of obtained star images is estimated to be within 10 milliseconds, resulting in star position accuracy of up to about 100 milliarcseconds, which is comparable with impact of other potential error sources.

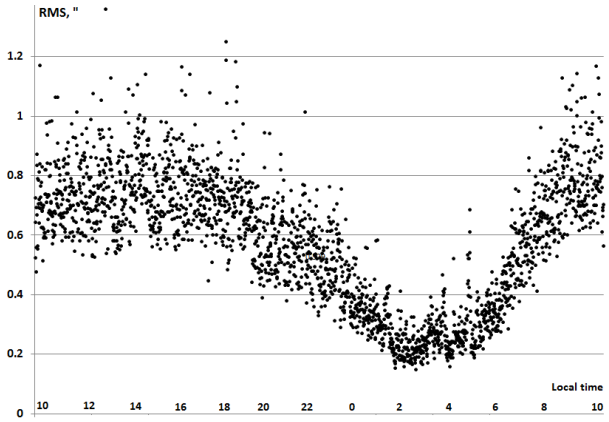

Fig. 3. RMS of tiltmeter position (estimated using series of 100 readings) during a day

Precision tiltmeter HRTM (Kahlmann et.al. 2004), used in camera, has 50 prad (~1e-5") resolution in ±2' range. Due to background vibrations, RMS of continuous series of readings varies from 2-3" inside building to 0.2..1" on a stable base in city (fig. 3), hopefully, in field conditions background vibrations will be less prominent.

If plumb line direction is calculated using a series of ~100 readings (obtained within 10 - 20 seconds), estimated direction accuracy should be well below 100 milliarcseconds (fig. 4).

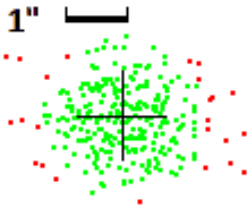

Fig. 4. Dispersion of tiltmeter readings (series of 100 readings at sampling rate 10 per second, rms=1.04")

Presently we estimate expected accuracy of vertical deflection values measured by prototype instrument at about 0.1"-0.2", of final configuration - better than 0.1". However, actual values of accuracy remain to be found.

3. Data model

The astrometric part of zenith camera takes images of near-zenith area. After identification of star images with reference catalog stars the place of projection of reference ellipsoid's normal to coordinate system of image can be determined. For this purpose, latitude and longitude of site, calculated using rectangular geocentric GNSS coordinates, representing normal to reference ellipsoid's surface, are used to calculate apparent places of stars.

NOVAS software package (Kahlman et.al. 1989) is the primary source of apparent places; it is possible also to use Starlink (Disney, Wallace 1985), which gives almost identical results.

In close vicinity of zenith, planar approximation of image coordinates is reasonably accurate (error in zenith distance z<5 milliarcseconds if z<0.25 dg and perpendicularity of image plane to zenith direction is within 0.25 dg); optical distortions and differential refraction in so small field also are very small. Besides, effect of these approximation errors on frame position is significantly compensated, if reference star distribution is close to symmetric around zenith. In planar approximation, dependency of rectangular image coordinates x_s, y_s on azimuth A_s and distance from ellipsoid normal's projection point z can be represented as:

$$x_S - x_{s0} = F * tg(z) * \sin(A-A_0),$$
$$y_S - y_{S0} = -F * tg(z) * \cos(A-A_0), \quad (1)$$

where x_{S0}, y_{S0} - projection of reference ellipsoid's normal to image plane, F - focus distance, A_0 - azimuth of image coordinate system's y axis negative direction; direction of y axis is down, as common for most imaging devices. If x_s, y_s are measured in image pixels, also F needs to be expressed in pixels. As pixel spacing value usually is not given with any accuracy estimations, in practice F must be determined as one of unknown variables. Such determination of F incorporates also part of

differential refraction and distortion effects.

Formula (1) can be solved if at least 2 stars are identified; calculations are iterative, convergence is fairly fast.

Processing of images (fig. 5) has demonstrated that typical frame model RMS is up to about 1/3 of pixel size (0.25" - 0.35" for current hardware configuration); it can be slightly better if image quality is good, but deteriorates down to 1"- 2" in conditions of strong convection, wind or background vibrations. If number of stars per frame is about 20, that gives frame position accuracy estimation in good conditions of up to 50-60 milliarcseconds.

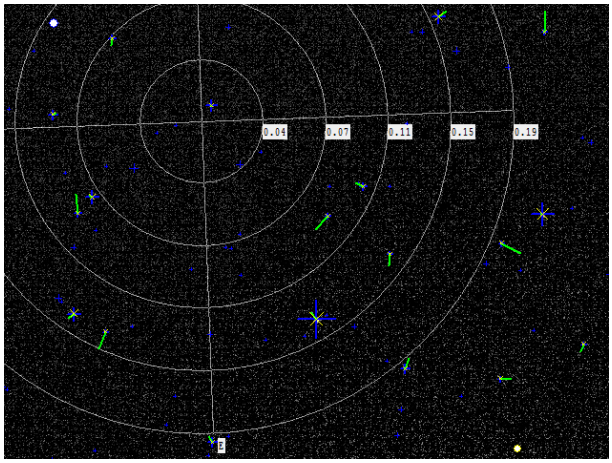

Fig. 5. Processed image of zenith area. Catalog stars (up to 13^m) are shown by vertical marks, image prototypes - by sloped marks, green lines represent approximation residuals

Tiltmeter measures coordinates of plumb line projection to tiltmeter coordinate plane x_t, y_t. Tiltmeter z axis orientation need to be adjusted close to both plumb line and instrument rotation axis directions, practically accuracy of adjustment will always be limited to vertical deflection value - at least several arc seconds. The tiltmeter coordinate system will be rotated by some angle A_t relative to imager coordinate system, this angle should be either made very small by careful adjustment, or measured with at least a few arcminute accuracy, observing both stars and plumb line direction while changing rotation axis direction within some vertical plane (for example, slightly inclining the mount).

Observations, made at different mount rotation azimuths A, gives series of plumb line and ellipsoid's normal positions in rotating coordinate systems of imager and tiltmeter. In case of ideal mount, trajectories of these positions would be circles, shifted from zero point:

$$X_{ZA} = X_{0A} + Rz * \sin(A_Z - A),$$

$$Y_{ZA} = Y_{0A} + Rz * \cos(A_Z - A), \qquad (2)$$

for projection of normal (X_{0A}, Y_{0A} depends on position of optical center on image and position of optical axis relative to rotation axis; R_Z - angle between ellipsoid's normal and rotation axis; Az - azimuth of ellipsoid's normal as seen from rotation axis).

Similarly,

$$X_{ZG} = X_{0G} + R_G \sin(A_G - A),$$

$$Y_{ZG} = Y_{0G} + R_G \cos(A_G - A), \qquad (3)$$

for tiltmeter zenith point (plumb line projection) (here R_G: angle between plumb line and rotation axis, A_G - azimuth of plumb line as seen from rotation axis, X_{0G} and Y_{0G} depend on position of tiltmeter Z axis relative to rotation axis).

Assuming that rotation axis for both trajectories is the same, difference between (2) and (3) (taking into account differences in orientation and scale of both involved coordinate systems) describes position of ellipsoid's normal relative to plumb line in rotating coordinate system:

$$X_{ZA} - X_{ZG} = x0 - \sin A * Y_D + \cos A * X_D,$$

$$Y_{ZA} - Y_{ZG} = y0 + \sin A * X_D + \cos A * Y_D, \qquad (4)$$

where X_D and Y_D: components of vertical deflection (angle from ellipsoid's normal to

plumb line) in topocentric coordinate system (Easting and Northing).

Formula (4) represents a circle in rotating (imager or tiltmeter) coordinate system (fig 6); size and phase of it is determined by vertical deflection value, position – by leveling of instrument and adjustment of its components. Formula (4) can be solved using standard least squares algorithm.

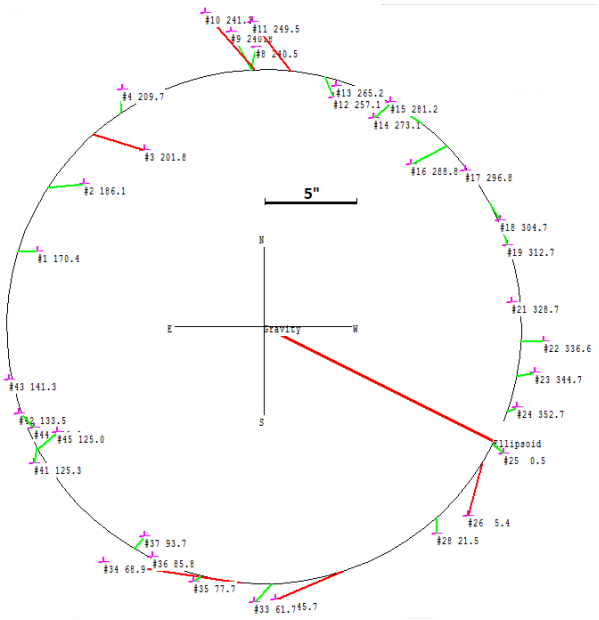

Fig. 6. Difference between directions to plumb line and to reference ellipsoid's normal in rotating coordinate system.

Unlike difference (4), individual behavior of (2) and (3) is affected by irregularities of support plane and bearings, possible changes in instrument orientation, modulating the ideal case circles with quite complex patterns. Properties of irregularities may be individual for each exemplar of mount. In particular, most of our prototype camera irregularities can be described as sum of two cylindrical deformations of the support plane with opposite directions of curvature, adding additional 3rd harmonic members in formulas (2) and (3) with amplitudes of about 33" and 2", resulting in zenith point trajectories like fig 7.

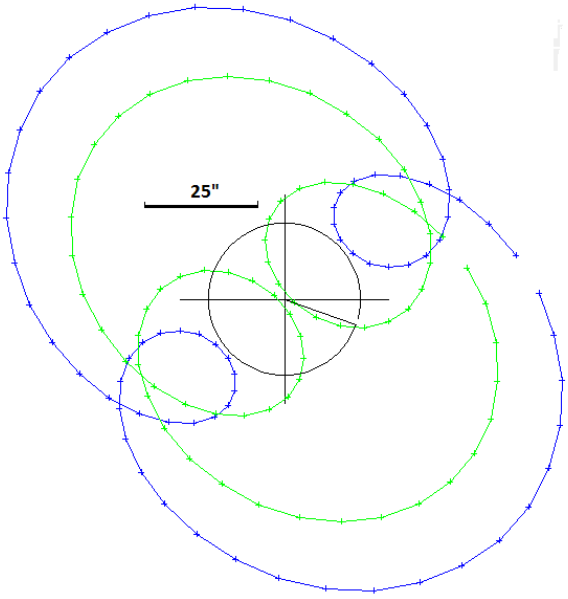

Fig. 7. Reference ellipsoid normal (blue) and plumb line direction (green) trajectories in rotating coordinate system and difference between them (black), representing their relative rotation.

4. Software

Our intention is to make the process of observations and data processing as automated, as possible. If instrument is properly adjusted and settings specified, the only action, needed to be done by operator, should be starting a session. Most of principal components for such operation mode are already in place. Nevertheless, we have an impression, that some manual quality control always will be necessary, therefore all processes can be controlled manually and are visualized whenever it was found helpful.

The control computer has Windows operating system. It should be equipped with and USB and wired and wireless (WiFi) communication devices for instrument control and data acquisition. Control program is written in C and uses several third party functional libraries - for hardware control

(actuators, stepper motors, imaging devices) and calculation of astrometric apparent places (NOVAS or StarLink).

Acknowledgement

The research was funded by ERAF, project Nr 2010/0207/2DP/2.1.1.1.0/10/APIA/VIAA/077

References

Featherstone, W.E. and Rüeger, J. 2000. The importance of using deviations of the vertical in the reduction of terrestrial survey data to a geocentric datum, The Trans-Tasman Surveyor, 1(3): 46-61. [Erratum in The Australian Surveyor 47(1): 7].

Featherstone, W.E.; Lichti, D.D. 2009. Fitting Gravimetric Geoid Models to Vertical Deflections, Journal of Geodesy 83(6): 583-589.

Hirt, C. 2006. Monitoring and Analysis of Anomalous Refraction Using a Digital Zenith Camera System. Astronomy and Astrophysics 459, 283-290.

Hirt, C.; Flury, J. 2008. Astronomical-topographic Levelling Using High-precision Astrogeodetic Vertical Deflections and Digital Terrain Model Data. Journal of Geodesy 82(4-5), 231-248.

Hirt, C.; Bürki, B.; Somieski, A.; Seeber, G. 2010. Modern Determination of Vertical Deflections using Digital Zenith Cameras. Journal of Surveying Engineering, Feb 2010, Vol. 136, No. 1, pp. 1-12.

Høg, E.; Fabricius, C.; Makarov, V.V.; Urban, S.; Corbin, T.; Wycoff, G.; Bastian, U.; Schwekendiek,P; Wicenec, A. 2000. The Tycho-2 Catalogue of the 2.5 Million Brightest Stars. Astronomy and Astrophysics 355, L27-L30.

Hirt C., Seeber, G. 2008 Accuracy Analysis of vertical deflection data observed with the Hannover Digital Zenith Camera System TZK2-D. Journal of Geodesy 82(6): 347 - 356.

Kudrys J. 2009. Automatic determination of the deflection of the vertical - first scientific results. Acta Geodynamics et Geomaterialia, Vol.6, No. 3 (155), 233-238.

Kudrys J. 2007. Automatic determination of vertical deflection components from GPS and zenithal star observations. Acta Geodyn. Geomater., Vol. 4., No 4 (148), 169-172.

Hirt, C.; Burki, B.; Guillaume, S.; Featherstone, W. 2010. Digital Zenith Cameras - State-of-the art Astrogeodetic Technology for Australian Geodesy. DIG Congress 2010, Sydney, Australia.

Gerstbach, G.; Pichler, H. 2003. A small CCD zenith camera (ZC-G) - developed for rapid geoid monitoring in difficult projects. Proceedings of XIII Nat. Conf of Yugoslav Astr., Oct. 17-20, 2002, Belgrade.

Ogriznovic V. 2009. A construction of an advanced measuring system for astro-geodetic determinations. Publ. Astron. Obs. Belgrade No 86 (2009), 145-150.

Halicioglu, K.; Deniz, R.; Ozener, H. 2012. Determination of Astro-geodetic vertical deflections using digital zenith camera system in Istanbul, Turkey. FIG working week 2012, Rome Italy, 5-10 may.

Kahlmann, T.; Hirt, C.; Ingensand, H. 2004. Hochpräzise Neigungsmessung mit dem elektronischen Einachspendelsystem HRTM. Ingenieurvermessung 2004, 14th International Conference on Engineering Surveying Zürich, 15. – 19. März 2004.

Kaplan, G. 2005. The IAU Resolutions on Astronomical Reference Systems, Time Scales, and Earth Rotation Models Explanation and Implementation. United States Naval Observatory circular No. 179. U.S. Naval Observatory, Washington, D.C.

Kaplan, G.; Hughes, J.; Seidelmann, P.; Smith, C.; Yallop, B. 1989. Mean and apparent place computations in the new IAU system. III. Apparent, topocentric and astrometric places of planets and stars. The Astronomical journal, Vol 97:1197-1210, Nr 4.

Disney, M.; Wallace, P. 1982. STARLINK. QJ Royal Astron. Soc. vol.23, p.485.

Zacharias, N.; Monet, D.; Levine, S.; Urban, S.; Gaume, R.; Wycoff, G. 2005. The Naval Observatory Merged Astrometric Dataset (NOMAD). www.nofs.navy.mil/nomad

Monet, D.; Levine, S.; Canzian, B.; Ables, H.; Bird, A.; Dahn, C.; Guetter, H.; Harris, H.; Henden, A.; Leggett, S.; Levison, H.; Luginbuhl, C.; Martini, J.; Monet, A.; Munn, J.; Pier, J.; Rhodes, A.; Riepe, B.; Sell, S.; Stone, R.; Vrba, F.; Walker, R.; Westerhout, G.; Brucato, R.; Reid, N.; Schoening, W.; Hartley, M.; Read, M.; Tritton,S. 2003. The USNO_B catalog. The Astronomical Journal, Vol 125, Nr 2: 984-9.